Synthesis, cytotoxicity, antioxidant activity and molecular modeling of new NSAIDs-EBS derivatives

Min Zhong, Ying Lu, Shaolei Li, Xiaolong Li, Zhenming Liu, Xianran He, Yongmin Zhang

Synthesis, cytotoxicity, antioxidant activity and molecular modeling of new NSAIDs-EBS derivatives

Min Zhong [a, b], Ying Lu [b], Shaolei Li [c], Xiaolong Li [c], Zhenming Liu [d], Xianran He [a, *], Yongmin Zhang [a, e, f *]

[a] *Wuhan Institute of Biomedical Sciences, School of Medicine, Jianghan University, Wuhan 430056, China*

[b] *Key Laboratory of Optoelectronic Chemical Materials and Devices, Jianghan University, Wuhan 430056, China*

[c] *Shenzhen Fushan Biological Technology Co., Ltd, Kexing Science Park A1 1005, Nanshan Zone, Shenzhen 518057, China*

[d] *State Key Laboratory of Natural and Biomimetic Drugs, School of Pharmaceutical Sciences, Peking University, Beijing 100191, China*

[e] *Sorbonne Université, CNRS, Institut Parisien de Chimie Moléculaire, UMR 8232, 4 Place Jussieu, 75005 Paris, France*

[f] *Key Laboratory of Tropical Medicinal Resource Chemistry of Ministry of Education, College of Chemistry and Chemical Engineering, Hainan Normal University, Haikou 571158, China*

*Corresponding author: Xianran He; Yongmin Zhang

E-mail: hexianran@163.com (Xianran He); yongmin.zhang@upmc.fr (Yongmin Zhang)

Abstract:

Two series of NSAIDs-EBS derivatives (**5a-j** and **9a-i**) based on the hybridization of nonsteroidal anti-inflammatory drugs (NSAIDs) skeleton and Ebselen moiety were synthesized. Their cytotoxicity was evaluated against five types of human cancer cell lines, BGC-823 (human gastric cancer cell line), SW480 (human colon adenocarcinoma cells), MCF-7 (human breast adenocarcinoma cells), HeLa (human cervical cancer cells), A549 (human lung carcinoma cells). Moreover, the most active compound **5j** showed IC_{50} values below 3 μM in all cancer cell lines and with remarkable anticancer activity against MCF-7 (1.5 μM) and HeLa (1.7 μM). The redox properties of the NSAIDs-EBS derivatives prepared herein were conducted by 2, 2-didiphenyl-1-picrylhydrazyl (DPPH), bleomycin dependent DNA damage and glutathione peroxidase (GPx)-like assays. Finally, TrxR1 inhibition activity assay and molecular docking study revealed NSAIDs-EBS derivatives could serve as potential TrxR1 inhibitor.

Keywords: Selenium; NSAIDs; Ebselen; Anticancer; Molecular modeling

Introduction

Non-steroidal anti-inflammatory drugs (NSAIDs) are a class of medications commonly used to treat symptoms of inflammatory diseases such as osteoarthritis and rheumatoid arthritis, and are routinely been used across the world [1, 2]. Moreover, numerous evidence from epidemiological and preclinical studies have shown that NSAIDs used in combination with different therapies, such as chemotherapy and immunotherapy or even radiation, represented an attractive strategy to increase anticancer efficacy and reduce toxicity [3-6]. Based on the fact that NSAIDs display their anticancer activities, the chemical modifications of their structures have demonstrated stronger cytotoxicity and chemo-preventive than corresponding NSAID alone [7, 8]. NSAIDs framework modification has become a structure-based medicinal chemistry strategy to design novel anticancer agents in the past decades [9-12].

Selenium is an essential trace mineral nutrient with multiple roles in the growth and function of living animal cells, and it effectively inhibits tumorigenesis in both animal models and epidemiological studies. Twenty-five selenoproteins in the human body exert specific biological functions. Selenium compounds have attracted huge interest in the past decades as chemotherapeutic and chemo-preventive agents. Several epidemiological studies have reported an inverse association between the nutritional selenium status and cancer risk. Specifically, selenazo compounds have received great attention owing to their chemical properties, pharmaceutical applications, and low toxicity [13-15]. Ebselen (EBS, **Fig 1**) is the most potential compound in cancer prevention, some EBS-related compounds have been reported to exhibit anticancer activity (**Fig 1)** [16-21].

In previous study, we have reported the synthesis of a series of novel NSAIDs-Selenium derivatives and screened their anticancer activity by *in vitro* study, the modification of NSAIDs scaffolds with Se functionalities (-SeCN, -Se-Se-, -$SeCF_3$) demonstrated potent inhibition of human tumor cell [22-25]. Because the pharmacological effects of Ebselen, including antioxidant and anticancer activities, twenty new NSAIDs-EBS derivatives were designed by the fusion of NSAIDs

fragment and Ebselen in a new molecule [**Fig 2**]. The hybrid compounds were evaluated for anticancer activities *in vitro*. Furthermore, the antioxidant potential of the compounds was investigated by employing DPPH, bleomycin-dependent DNA damage and GPx-like assays. Finally, Thioredoxin Reductase (TrxR1) inhibition activity assay and molecular docking study (TrxR1 as docking protein) were performed, in order to predict the target and anticancer activity of the prepared NSAIDs-EBS hybrid compounds.

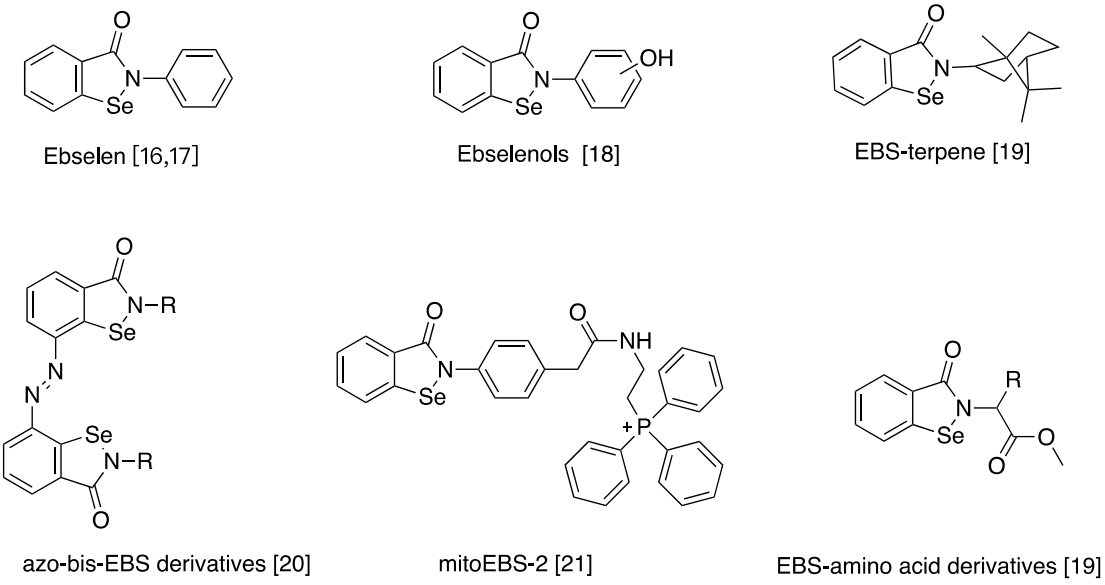

Fig. 1. EBS-related compounds with anticancer activity

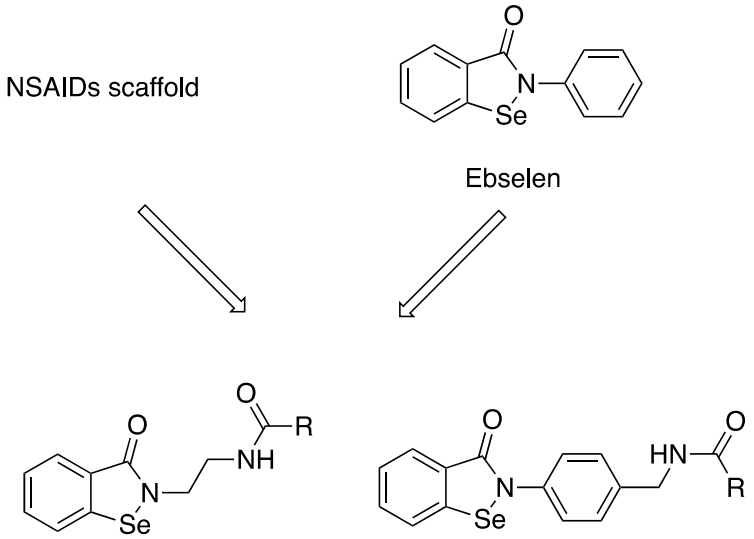

Fig. 2. NSAIDs-EBS derivatives

2. Results and Discussion

2.1 Chemistry

The synthesis strategies of compounds **5a-j** are outlined in Scheme **1**. First, 4-aminobenzylamine reacted with di-tert-butyl dicarbonate to give intermediate **1**. The reactions of **1** with o-iodobenzoyl chloride in the present of TEM provided compound **2**. The reaction of **2** with KSeCN and following deprotection produced the EBS intermediate **4**. Finally, the target products **5a-j** were obtained by reacting compound **4** with commercially available NSAIDs in the present of EDCI and HOBt as condensation agent (**Scheme 1**).

The synthesis of target compounds **9a-i** is shown in Scheme **2**. The reaction of o-iodobenzoyl chloride with tert-butyl (2-aminoethyl) carbamate afforded the intermediate **6**. Compound **6** was reacted with KSeCN and following deprotection produced the EBS intermediate **8**. Finally, the target products **9a-i** were obtained by reacting compound **8** with commercially available NSAIDs in the present of EDCI and HOBt as condensation agent (**Scheme 2**).

The purity of all final compounds was 95% or higher and their chemical structures were characterized using ^{1}H NMR, ^{13}C NMR and HRMS (ESI).

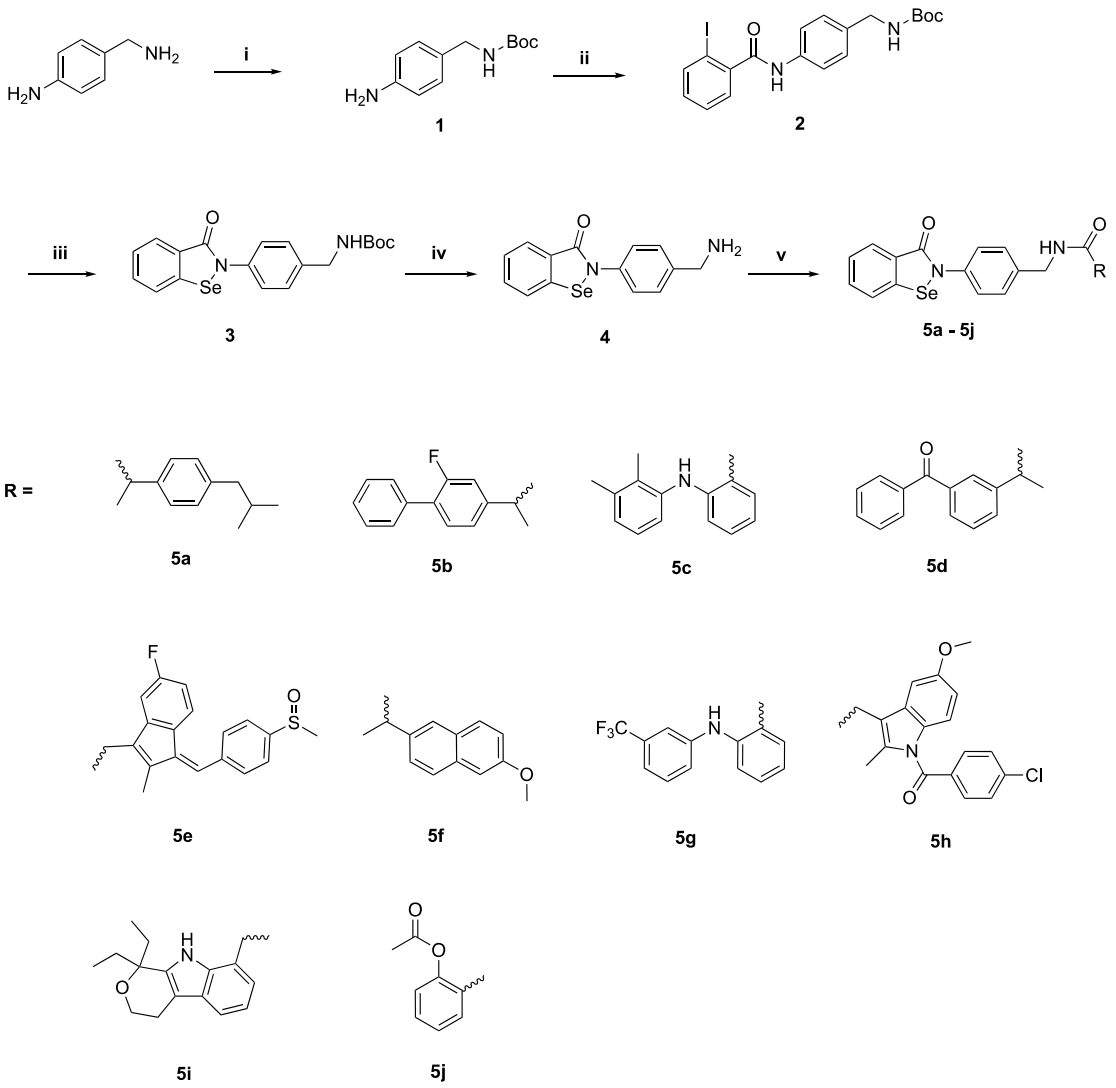

Scheme 1. i) $(Boc)_2O$, THF, 0-25 °C; ii) TEA, DCM, 25 °C; iii) CuI, Cs_2CO_3, KSeCN, 1,10-phenanthroline, DMF, 100 °C; iv) TFA, DCM, r. t.; v) NSAIDs, EDCI, HOBT, TEA, DCM.

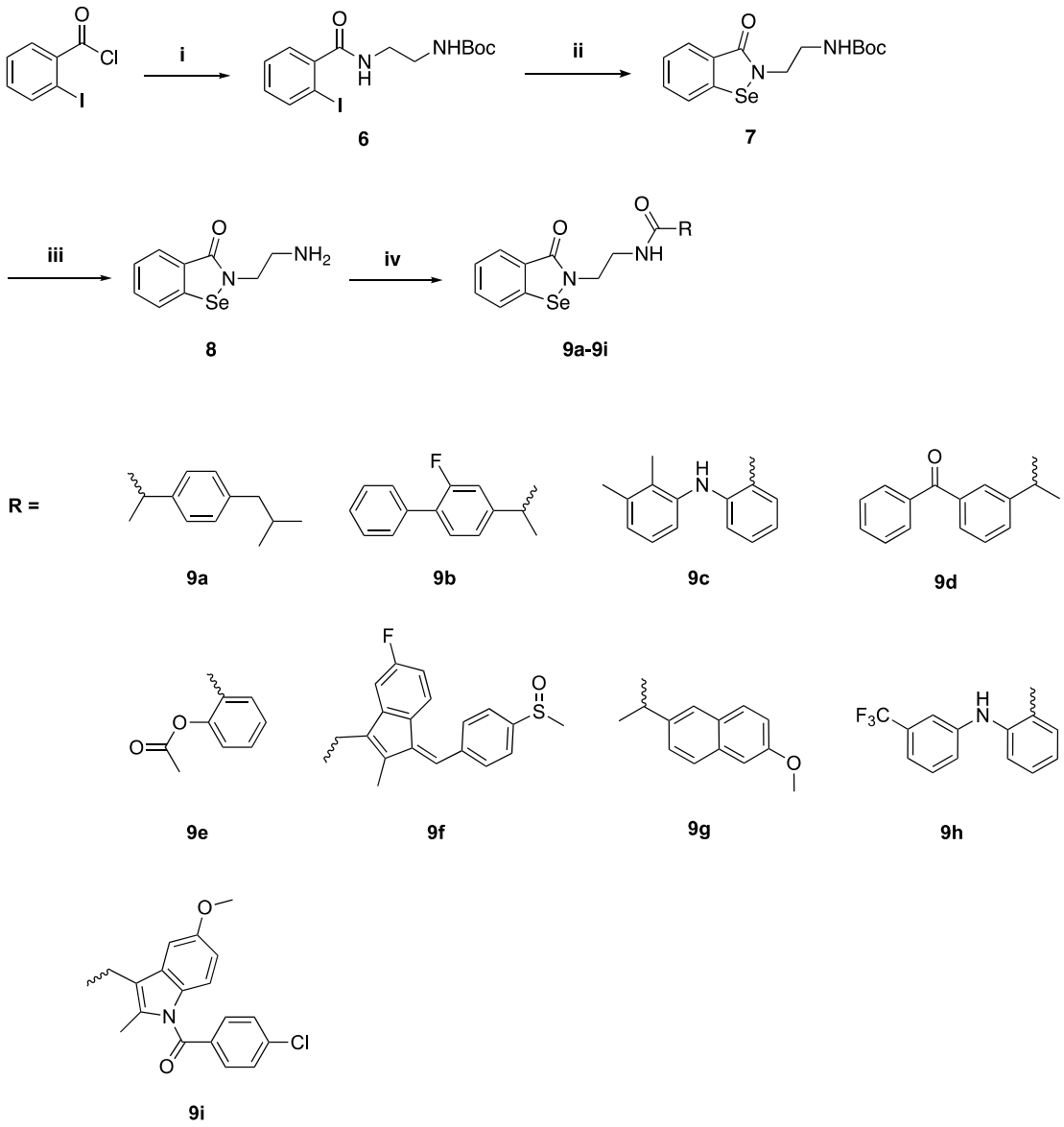

Scheme 2. i) N-Boc-ethylenediamine, TEA, DCM, 0°C; ii) CuI, Cs_2CO_3, KSeCN, 1,10-phenanthroline, DMF, 100 °C; iii) TFA, DCM, 25 °C; iv) NSAIDs, EDCI, HOBT, TEA, DCM, 25 °C.

2.2. Cytotoxicity

MTT (3-(4,5- dimethylthiazol-2-yl)-2,5-diphenyltetrazolium bromide) assay was conducted to evaluate the potential antiproliferative activities against human tumor cell lines derived from various human cancer types: BGC-823 (human gastric cancer cell line), SW480 (human colon adenocarcinoma cells), MCF-7 (human breast

adenocarcinoma cells), HeLa (human cervical cancer cells), A549 (human lung carcinoma cells) of target compounds **5a-j** and **9a-i**, doxorubicin was selected as reference standard (Table **1**).

As shown in **Table 1**, most of the NSAIDs-EBS derivatives exhibited good antiproliferative activity with IC_{50} values at micromolar level, while the selected patent NSAIDs (Aspirin, Ibuprofen and Naproxen) and Ebselen are inactive against all cells even in the maximum dose of 50 μM. The IC_{50} values obtained for the NSAIDs-EBS derivatives showed that the fusion of NSAIDs scaffold and ebselen moiety in a new molecule result in the significant effect on cancer cell line.

The results in table **1** showed that the cytotoxic activity of NSAIDs-EBS derivatives containing a phenyl moiety between two nitrogen atom (**5a-i**) is better than corresponding NSAIDs-EBS derivatives containing ethyl moiety (**9a-i**), considering the lipophilicity and electron withdrawing effect.

Furthermore, the cytotoxic activity of compounds **5a, 5b, 5c, 5d, 5e, 5g, 5h, 5i** and **5j** displayed IC_{50} values below 10 μM against BGC-823 cells. The most active compounds of these two series are **5c** and **5j**. These two compounds show IC_{50} values below 5 μM in all of tested cancer cell lines. Compound **5j** emerges the most potent agent with IC_{50} values below 3 μM in all cancer cell lines and with remarkable anticancer activity against MCF-7 (1.5 μM) and HeLa (1.7 μM).

Table 1. Cytotoxic activity expressed by IC_{50} of NSAIDs-EBS derivatives (**5a-j** and **9a-i**) on different cancer cell lines.

Compound	IC_{50}(μM)[a]				
	BGC-823	**SW-480**	**MCF-7**	**HeLa**	**A549**
Aspirin[b]	>50	>50	>50	>50	>50
Ibuprofen[b]	>50	>50	>50	>50	>50
Naproxen[b]	>50	>50	>50	>50	>50
Ebselen[b]	>50	>50	>50	>50	>50
5a	7.5±0.7	10.4±1.1	12.4±1.2	9.3±0.8	8.1±0.8
5b	6.5±0.4	8.3±0.8	11.3±1.1	9.5±0.9	12.3±1.2
5c	3.4±0.2	4.5±0.4	4.2±0.3	3.8±0.2	3.6±0.2
5d	11.2±1.2	12.5±1.2	8.4±0.8	9.2±0.9	13.2±1.3
5e	9.5±0.9	9.8±0.9	7.4±0.7	8.4±0.8	8.3±0.8
5f	13.5±1.3	7.4±0.7	13.8±1.3	9.7±0.9	11.4±1.1
5g	8.4±0.8	13.7±1.2	14.2±1.1	7.5±1.3	12.7±1.2
5h	9.2±0.9	7.5±0.7	11.3±1.1	14.3±1.4	10.3±1.0
5i	9.8±1.5	12.3±1.2	8.8±0.7	12.6±1.3	9.8±0.9
5j	2.4±0.2	2.8±0.2	1.5±0.1	1.7±0.1	2.1±0.2
9a	12.5±1.2	11.4±1.1	15.7±1.5	10.6±1.1	9.4±0.8
9b	9.5±0.6	11.3±1.1	14.9±1.4	10.4±1.0	13.6±1.3
9c	6.5±0.7	7.2±0.7	5.3±0.5	8.8±0.8	5.2±0.5
9d	13.6±1.4	14.6±1.5	10.3±1.0	11.3±1.1	15.6±1.5
9e	11.4±1.1	14.2±1.4	14.5±1.4	12.7±1.2	10.6±1.0
9f	16.6±1.6	10.4±1.0	14.4±1.4	11.3±1.1	13.3±1.3
9g	13.5±1.3	15.7±1.5	16.5±1.6	8.8±0.8	14.7±1.4
9h	11.4±1.1	9.4±0.9	12.6±1.2	15.2±1.5	12.2±1.2
9i	17.4±1.7	14.3±1.4	10.3±1.0	13.6±1.3	11.2±1.1
Doxorubicin[c]	9.8±0.9	12.4±1.2	12.8±1.2	11.5±1.1	9.4±0.9

[a] IC_{50} values are indicated as the mean ± SD (standard error) of at least three independent experiments.

[b] Patent NSAIDs and Ebselen.

[c] Standard benchmark compound.

2.3. Antioxidant activity

Reactive Oxygen Species (ROS) is actually a collective term that is used to describe oxygen-derived small and highly reactive molecules, such as superoxide anion (O2-), hydroxyl radical (OH·), peroxyl radical (ROO·) and alkoxyl radical (RO·) [26]. ROS play essential roles in altering protein structure, thereby changing its function and participate in many pathological processes [27]. Various human diseases, including different types of cancer, are associated with a disturbed intracellular redox balance and oxidative stress (OS) [28].

Owing to the fact that a number of synthetic organoselenium compounds have been synthesized for their use as redox-modulators in the last few years [29], the antioxidant activity of compounds (**5c, 5j**) are further estimated employing different biochemical assays such as DPPH, bleomycin-dependent DNA damage and Gpx-like assays [30].

2.3.1. Radical scavenging capacity (DPPH) assay.

The DPPH chemical assay is considered to be the rapid tools to evaluate the radical-scavenging capability of organic selenides [31]. The antioxidant activity of a compound is checked by its ability to decolorize $DPPH^{\cdot}$ radical (purple color in methanol) to DPPHH (colorless) and the corresponding radical-scavenging activity is estimated by the decrease in the absorbance at 517 nm [32]. Vitamin C was used as a positive control (**Table 2**). Antioxidant activity was calculated as follows:

$$\%\ \text{Antioxidant activity} = [(\text{control absorbance} - \text{sample absorbance}) / \text{control absorbance}] \times 100\%$$

As shown in **Table 2**, NSAIDs-EBS derivatives **5f** and **5h** were the most active compounds in this assay, demonstrating a good free-radical scavenging activity compared to Vitamin C.

2.3.2. Bleomycin DNA damage assay.

Bleomycin (BLM) is a radiomimetic antitumor antibiotic first isolated from *Streptomyces verticillus* [33]. BLM is widely used in clinical chemotherapy for the treatment of different types of cancer, namely testicular cancer, lymphoma, lung cancer, cervical cancer and cancers of the head and neck [34-35]. The bleomycin-iron DNA damage assay has been routinely used as a preliminary method to test potential of drugs and organic selenium compound [36]. As shown in **Table 2**, compounds **5a**, **5h, 5j** and **9g** induced DNA degradation significantly more than other tested compounds.

Table 2 Redox modulation activity of NSAID-EBS derivatives.

Compd. No.	DPPH assay		Bleomycin-dependent DNA damage assay
	Inhibition %	Fold	Absorbance
Vitamin C	97.2±1.3	1	292±2.73
5a	42.6±2.3	0.4	106.3±0.43
5b	58.2±3.6	0.6	57.3±0.33
5c	54.3±4.6	0.5	72.4±0.33
5d	31.3±2.9	0.3	85.3±1.67
5e	42.9±2.1`	0.4	72.4±0.52
5f	68.6±2.7	0.7	82.8±0.84
5g	51.5±1.2	0.5	56.1±0.41
5h	78.7±3.3	0.8	101.3±1.51
5i	52.1±4.3	0.5	97.4±1.45
5j	57.3±3.1	0.5	108.3±0.39
9a	33.5±2.1	0.3	68.4±1.32
9b	42.5±2.4	0.4	85.7±2.12
9c	37.4±2.1	0.4	72.4±1.33
9d	33.3±1.6	0.3	87.6±1.20
9e	41.4±2.2	0.4	91.4±1.27
9f	29.0±1.0	0.3	68.4±1.33
9g	28.6±2.6	0.3	123.1±2.47
9h	41.7±2.0	0.4	77.7±1.32
9i	27.3±2.3	0.3	92.4±1.26

2.3.3. Glutathione peroxidase-like activity.

Glutathione peroxidase (GPx) is a selenoprotein that protects cells by catalyzing the reduction of peroxides with the stoichiometric reductant glutathione (GSH) [37]. The GPx activity of NSAIDs-EBS derivatives was estimated by the decrease in absorbance (340 nm) due to the oxidation of NADPH to $NADP^+$. Ebselen was used as the positive control.

The results shown in **Fig. 3** indicated that compounds **5a**, **5b**, **5c**, **5f**, **5h**, **5j** and **9f** displayed a GPx-like activity better than other derivatives. Compounds **9a-i**, for which the linker is ethyl group between NSAIDs fragment and Ebselen moiety, exhibited weaker GPx-like activity than that of phenyl group as linker except compound **9f**. Compound **5j** was the most active derivatives in this assay, up to 3 fold to the GPx mimetic ebselen.

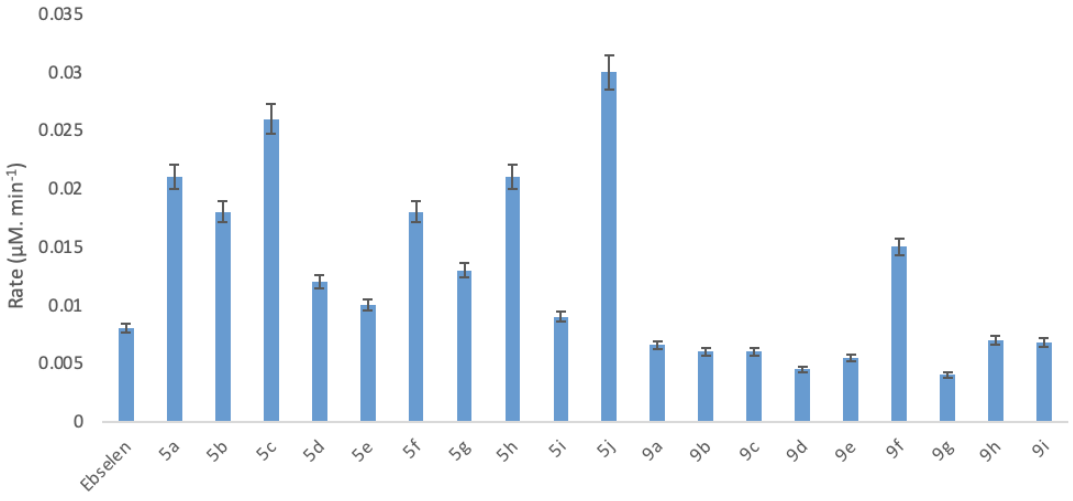

Fig. 3. GPx-like activity assay of NSAID-EBS hybrid compounds in μM. Min^{-1}.

2.4. TrxR1 inhibition activity.

The principle of enzyme inhibition experiment is that DTNB [5,5 '-dithiobis - (2-nitrobenzoic acid)] is one of the substrates of TrxR1. In vitro experiments, DTNB will be decomposed into TNB (2-nitro-5-thiobenzoic acid) by TrxR1 in the presence of NADPH. TNB has specific UV absorption at 412 nm. Therefore, the reaction rate of enzymatic decomposition reaction can be reflected by measuring the UV absorption at 412 nm per unit time of the reaction system, and then measuring enzyme activity [38]. Auranofin was used as the positive control.

As shown in Table **3**, all NSAIDs-EBS derivatives exhibited strong inhibition against TrxR1, compounds **5a, 5b, 5c, 5d, 5e, 5f, 5g, 5h, 5i** and **5j** shown EC_{50} values below 20 nm, which is better than Auranofin. The result showed compound **5a-j** have potential candidate as inhibitor of TrxR1.

Table 3 TrxR1 inhibion activity of NASIDs-EBS derivatives

Compd. No.	TrxR1 EC_{50} (μM)
5a	17.2±1.38
5b	11.2±1.87
5c	14.3±0.85
5d	19.6±1.72
5e	10.4±1.42
5f	14.6±1.34
5g	11.5±1.21
5h	15.7±1.33
5i	17.1±2.31
5j	8.8±0.43
9a	23.5±3.11
9b	28.5±2.82
9c	26.6±2.23
9d	23.6±1.25
9e	21.4±2.21
9f	27.0±1.34
9g	28.4±2.61
9h	24.8±2.53
9i	24.5±2.42
Auranofin	22.4±1.62

2.5. Docking Studies

The binding mode between organoselenium compounds and Mammalian TrxR1 protein was described by docking studies. TrxR1 consists of several functional domains, including FAD and NAD binding domains at the N-terminal, and the dimerization interface domain at the flexible C-terminal side [39-41]. It has been reported that flexible docking can simulate the interaction between small molecules and TrxR1[4]. Therefore, compounds **5c** and **5j** were docked into the TrxR1 protein (PDB id: 1H6V) using Flexible Docking Protocol as reported in the literature [42].

The distances between the selenium atom of all two compounds and Cys497/Cys498 of TrxR1 were measured and focused on because it is closely related to the accessibility of cysteine thiol attack selenides. These compounds showed acceptable docking results (**Table 4-5**).

For compound **5j**, pose 4 showed a good docking conformation with the relatively high value of -CDOCKER energy (12.562 kcal/mol) and a relatively close distance between the selenium atom and Cys498 (9.773 Å) (**Table 5,** Pose 4). This good conformation may be related to the key hydrogen bond interaction between the oxygen of acetyl group and SER483 (2.29 Å). In addition, hydrogen bonding between the oxygen of 3-oxobenzo[d][1,2]selenazol-2(3H)-yl)benzyl and TRP407 (2.00 Å) is also important (**Figure 5**). Although the pose 5 of compound **5c** showed no hydrogen bond, it had an acceptable value of -CDOCKER energy (7.350 kcal/mol) and distance between the selenium atom and Cys498 (6.614 Å). There were many hydrophobic interactions, including hydrophobic (Pi-Alkyl) between two different benzene rings and CYS498 (5.141 Å, 5.137 Å), hydrophobic (Alkyl) between methyl groups on benzene ring and CYS498 (4.190 Å), and hydrophobic (Pi-Alkyl) between phenyl of 3-oxobenzo[d][1,2]selenazol-2(3H)-yl)benzyl and LEU409 (5.469 Å) (**Table 4,** Pose 5; **Figure 4**).

Table 4 Ligand-protein poses for compound **5c**

Pose Index	CDOCKER_ENERGY	CDOCKER_INTERRATION_ENERGY	LibDock Score	LibDock Pose	Distance Cys497Se	Distance Cys498Se
1	13.2384	45.4329	61.7485	7	22.446	17.008
2	10.4149	43.5291	66.0141	6	20.851	22.024
3	9.7976	42.6044	62.2043	8	12.735	5.175
4	8.60531	40.4135	69.1193	2	22.848	20.817
5	7.34978	39.2558	87.5773	4	8.561	6.614
6	7.09795	41.2406	72.2109	5	11.294	8.087
7	7.06524	40.4968	83.4649	5	11.488	8.983
8	6.99063	38.2927	53.7714	7	11.280	14.775
9	6.84262	41.0232	69.3691	7	11.386	7.247
10	6.65588	39.1307	96.9686	1	14.168	8.893
11	6.35112	38.4162	71.5831	1	12.521	4.748
12	6.35059	38.618	81.4432	6	12.000	7.920
13	5.98894	39.1252	63.7073	3	21.559	19.587
14	5.54376	38.0319	53.3036	10	11.086	7.030
15	4.873	39.0683	57.8956	4	8.054	10.010
16	4.61831	36.9053	102.476	1	7.777	5.214
17	4.43294	38.7698	61.2802	4	15.480	8.839
18	4.25345	36.326	78.3978	1	12.174	6.446
19	3.82841	35.5458	64.8576	2	5.041	7.519

20	3.42857	38.0731	99.8759	2	7.867	4.961
21	3.34678	36.3131	62.9525	10	6.237	8.013
22	2.84919	37.2215	67.7144	4	14.199	11.248
23	2.75952	34.6775	56.7099	8	22.439	19.095
24	2.39014	34.6317	63.1427	10	12.714	8.074
25	1.69794	35.5682	65.1989	8	8.839	9.121
26	1.65597	34.7061	68.534	3	19.010	21.709
27	0.761431	33.8651	59.5824	9	14.171	9.310
28	0.457764	32.3594	54.8453	10	12.305	7.603
29	0.102792	31.8219	65.1714	9	10.777	5.253
30	-4.37105	26.9452	55.4452	10	9.992	6.198
31	-4.9625	30.776	59.7369	3	3.255	8.833
32	-6.46586	28.6328	71.1944	8	10.521	7.237

Table 5 Ligand-protein poses for compound **5j**

Pose Index	-CDOCKER_ENERGY	-CDOCKER_INTERRATION_ENERGY	LibDockScore	LibDock Pose	Distance Cys497Se	Distance Cys498Se
1	19.8943	44.2099	64.1592	6	9.110	6.912
2	19.1219	46.7132	70.4112	6	20.387	32.317
3	18.4552	43.1668	78.5763	5	11.084	11.073
4	17.5838	42.5621	63.3701	8	7.990	6.253
5	17.4763	41.6662	54.3429	8	13.337	7.076
6	17.4124	43.2487	75.6808	4	9.017	8.893
7	16.1704	39.5507	56.622	9	9.765	6.149
8	15.7242	40.3922	83.1296	2	8.880	8.007
9	15.2206	40.1879	76.0685	3	15.860	12.024
10	15.2121	40.9488	86.7815	1	10.155	7.855
11	14.0462	39.2595	77.2953	6	12.905	6.510
12	13.9291	38.1134	73.0708	5	10.329	9.048
13	13.3664	38.6014	76.3795	7	10.564	3.642
14	13.1608	39.1776	73.2676	8	13.721	12.239
15	12.7202	38.1457	98.5742	1	13.135	6.068
16	12.7057	37.448	87.1604	1	11.449	9.654
17	12.5957	37.812	61.7665	7	13.710	6.822
18	12.0462	37.1745	79.0099	4	9.027	7.055
19	11.8174	37.5311	102.361	1	9.922	9.167
20	11.7229	37.8333	79.1876	3	11.555	8.871
21	11.5495	36.7249	59.7242	9	12.927	9.550
22	11.46	36.1866	73.0299	6	20.179	18.749
23	11.0925	34.6597	67.1314	10	10.872	8.150
24	9.93392	33.6135	91.6464	3	9.116	7.502
25	9.76676	38.4745	58.9347	8	9.822	10.982
26	7.13759	35.5936	71.6435	9	11.223	8.436
27	5.71796	32.2846	69.6629	10	8.831	7.709
28	5.05737	30.4126	65.6731	8	12.929	7.701
29	2.94544	30.5268	54.4481	10	10.113	6.789
30	1.81129	26.1195	51.8166	9	20.884	21.979

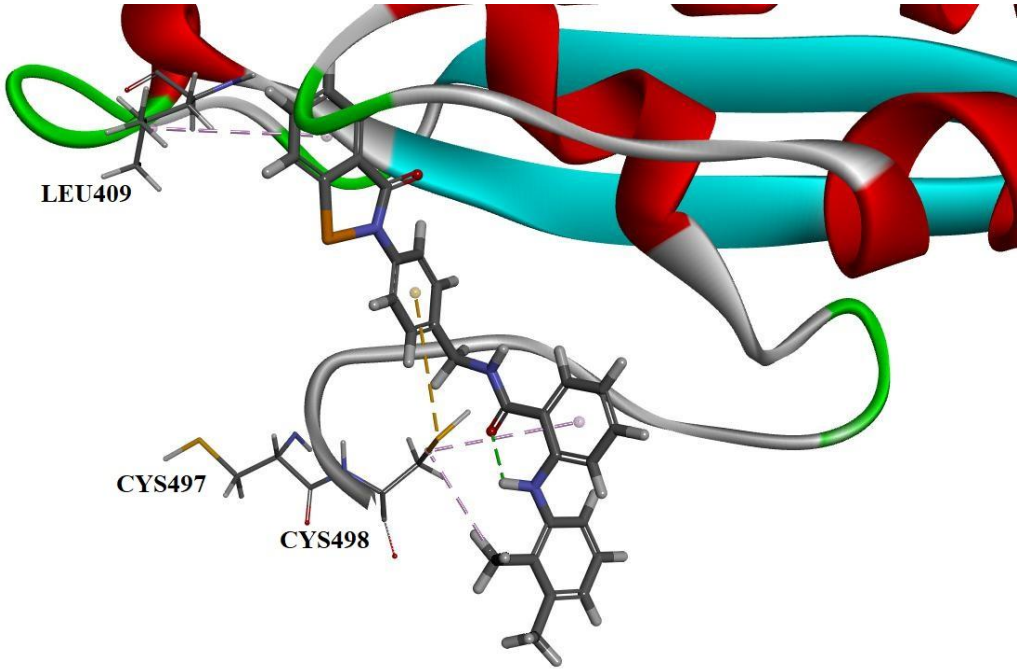

Fig. 4. The pose 5 of **5c**. Four interactions were shown: Hydrophobic (Pi-Alkyl) between two different benzene rings and CYS498 (5.141 Å, 5.137 Å), hydrophobic (Alkyl) between methyl groups on benzene ring and CYS498 (4.190 Å), and hydrophobic (Pi-Alkyl) between phenyl of 3-oxobenzo[d][1,2]selenazol-2(3H)-yl)benzyl and LEU409 (5.469 Å).

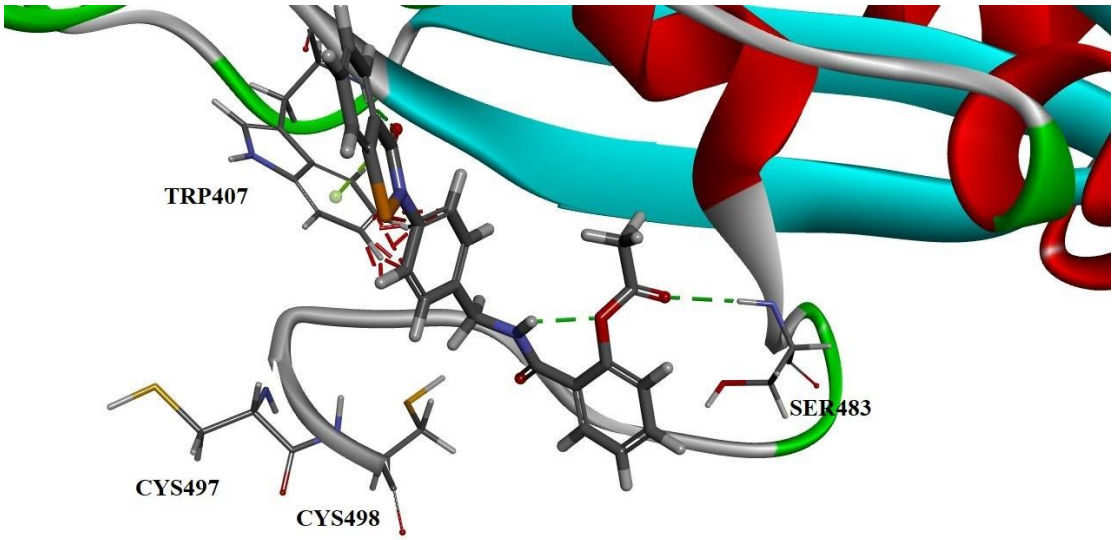

Fig. 5. The pose 4 of **5j**. Two interactions were shown: hydrogen bonding between the oxygen of acetyl group and SER483 (2.29 Å)and hydrogen bonding between the oxygen of 3-oxobenzo[d][1,2]selenazol-2(3H)-yl)benzyl and TRP407 (2.00 Å).

3. Conclusions

In summary, two series of NSAIDs-EBS derivatives were synthesized and characterized. Five human cell lines (BGC-823, SW480, MCF-7, HeLa and A549) were selected to test cytotoxicity of the compounds. Compound **5j** showed most potent cytotoxicity activity with IC_{50} values below 3μm against five cancer cell lines. Moreover, most of the NSAIDs-EBS derivatives exhibited moderate to good CPx-like activity compared to ebselen. Finally, TrxR1 inhibition activity assay and in flexible docking study performed into TrxR1 enzyme, compound **5j** showed a moderate binding energies and binding mode that the distance between the selenium atom and Cys497/Cys498.

Overall, considering the potency of these NSAIDs-EBS derivatives on cancer cell viability, antioxidant activity and docking assay, the further study will focus on design of this new type of potential NSAIDs-EBS anticancer agents.

4. Experimental section

4.1. General methods

All chemical reagents for the synthesis of the compounds were purchased from Macklin (Shanghai, China) or TCI (Shanghai, China) and used without further purification unless stated otherwise. Thin-layer chromatography (TLC) was performed on aluminium pre-coated sheets (E. Merck Silica gel 60 F254). Melting points were recorded on an Electrothermal apparatus and are uncorrected. NMR spectra were recorded in $CDCl_3$ on a Bruker Avance 400 MHz (for ^{1}H) and 100 MHz (for ^{13}C) spectrometer with 5 mm PABBO probe. The following abbreviations were used to explain the multiplicities: s = singlet, d = doublet, t = triplet, q = quartet, and m = multiplet. Chemical shifts (δ) are reported in parts per million (ppm) downfield from TMS and the coupling constants (*J*) are expressed in Hertz (Hz). High-resolution MS were performed on a SCIEX，TripleTOF 5600+, operating in ionization mode.

4.2. Experimental procedures

*4.2.1. Procedure for the synthesis of compound **1***

To a solution of 2-(4-aminophenyl)ethylamine (2.0 g) in THF (20 mL) was added $(Boc)_2O$ (4.3 g) at 0°C. Then the mixture was stirred at 25°C for 3 hrs. TLC showed the reaction was complete. The mixture was concentrated under reduced pressure. The crude product was purified by column chromatography on silica gel (PE/EA = 50:1 to 5:1) to afford compound **2** as white solid (2 g) in 55% yield. ^{1}H NMR (400 MHz, $CDCl_3$): 1.45 (s, 9H, 3-CH_3), 3.66 (br, 2H, -NH), 4.18 (d, J = 5.8 Hz, 2H, -CH_2), 4.73 (br, 1H, -NH), 6.66-6.61 (m, 2H), 7.10-7.03 (m, 2H). ^{13}C NMR (100 MHz, $CDCl_3$): 28.6, 44.5, 79.4, 115.3, 128.9, 129.0, 145.8.

*4.2.2. procedure for the synthesis of compound **2***

To a solution of compound **1** (2.0 g) in DCM (40 mL) was added TEA (1.36 g) at 0°C, then 3 (1.36 g) was added slowly into the mixture. The mixture was stirred at 25°C for 0.5 hour. TLC showed the reaction was complete. The mixture was diluted with H_2O (40 mL), the aqueous layer was extracted with DCM (20 mL×2), the combined organic layer was washed with brine (20 mL× 2), dried over Na_2SO_4, filtered and the filtrate was concentrated under reduced pressure. The crude product was purified by beating (DCM/MeOH=4:1) to afford compound **2** (2.8 g) as a white solid in 69% yield. ^{1}H NMR (400 MHz, $CDCl_3$): 1.45 (s, 9H, 3-CH_3), 4.28 (s, 2H, -CH_2), 4.90 (brs, 1H, -NH), 7.14 (t, 1H, J = 8.00 Hz, ArH), 7.28 (s, 1H, ArH), 7.41 (t, 1H, J = 8.00 Hz, ArH), 7.50 (d, 1H, J = 8.00 Hz, ArH), 7.59 (d, 2H, J = 8.00 Hz, ArH), 7.68 (brs, 1H, ArH), 7.89 (d, 1H, J = 8.00 Hz, ArH). ^{13}C NMR (100 MHz, $CDCl_3$): 28.4, 44.7, 79.8, 92.7, 115.3, 127.7, 128.9, 129.0,130.9, 131.3, 141.7, 142.5, 145.8, 164.9.

*4.2.3. procedure for the synthesis of compound **3***

To a solution of compound **2** (1.9 g) in DMF (18 mL) was added CuI (799 mg), Cs_2CO_3 (3.43 g), KSeCN (726 mg) and 1,10-phenanthroline (757 mg). Then the mixture was stirred at 100 °C for 0.5 hour. TLC showed the reaction was complete. The mixture was cooled to 25°C and then diluted with H_2O (40 mL) and ethyl acetate （EA）(20 mL), the aqueous layer was extracted with EA (20 mL×2), the combined organic layer was washed with brine (20 mL×2), dried over Na_2SO_4, filtered and the

filtrate was concentrated under reduced pressure. The crude product was purified by beating (MeOH, 5mL) to afford compound 3 (0.83 g) as a yellow solid in 49% yield. ^{1}H NMR (400 MHz, DMSO): 1.41 (s, 9H, 3-CH_3), 4.14 (s, 2H, -CH_2), 7.31 (d, 1H, J = 8.00 Hz, ArH), 7.45-7.50 (m, 2H, ArH), 7.57 (d, 1H, J = 8.00 Hz, ArH), 7.68 (t, 1H, J = 8.00 Hz, ArH), 7.91 (d, 1H, J = 8.00 Hz, ArH), 8.09 (d, 1H, J = 8.00 Hz, ArH). ^{13}C NMR (100 MHz, DMSO): 28.7, 44.9, 79.6, 121.4, 127.1, 127.5, 128.8, 131.1, 131.4, 133.8, 136.2, 137.4, 143.2, 167.6.

*4.2.4. procedure for the synthesis of compound **4***

To a solution of compound 3 (430 mg) in DCM (5 mL) was added TFA (1 mL). The mixture was stirred at 25°C for 1 hour. TLC showed the reaction was complete. The mixture was concentrated under reduced pressure to afford crude compound **4**. The pH of crude was adjusted to about value 9 by TEA. The mixture was used for the next step without purification.

*4.2.5. General procedure for the synthesis of compounds **5a-5j***

To a solution of patent NSAIDs (1.0 eq) in DCM (5 mL) was added EDCI (1.2 eq.), HOBT (1.2 eq.) and TEA (3.0 eq.) and compound 4 (1.0 eq). The mixture was stirred at 25°C for 16 hrs. TLC showed the reaction was complete. The mixture was diluted with H_2O, the aqueous layer was extracted with DCM, the combined organic layer was washed with brine, dried over Na_2SO_4, filtered and the filtrate was concentrated under reduced pressure. The crude product was purified by beating to afford the desired product.

4.2.5.1. 2-(4-isobutylphenyl)-N-(4-(3-oxobenzo[d][1,2]selenazol-2(3H)-yl)benzyl) Propenamide **(5a)**.

Yield: 85 %. White solid. Mp: 103-105°C. ^{1}H NMR (400 MHz, DMSO-6d): δ 0.85 (d, 6H, J = 4.00 Hz, 2-CH_3), 1.36 (d, 3H, J = 8.00 Hz, -CH_3), 1.77-1.84 (m, 1H, -CH), 2.41 (d, 2H, J = 8.00 Hz, -CH_2), 3.65 (q, 1H, J = 8.00 Hz, -CH), 4.26 (d, 2H, J = 8.00 Hz, -CH_2), 7.09 (d, 2H, J = 8.00 Hz, ArH), 7.21 (d, 2H, J = 8.00 Hz, ArH), 7.25 (d,

2H, J = 8.00 Hz, ArH), 7.47 (d, 1H, J = 8.00 Hz, ArH), 7.52 (d, 2H, J = 8.00 Hz, ArH), 7.66-7.70 (m, 1H, ArH), 7.89-7.91 (m, 1H, ArH), 8.10 (d, 1H, J = 8.00 Hz, ArH), 8.47-8.50 (m, 1H, -NH). ^{13}C NMR (100 MHz, DMSO-6d): δ 18.9, 22.6, 30.1, 42.1, 44.7, 45.3, 125.0, 126.3, 126.7, 127.5, 128.2, 128.4, 129.0, 129.3, 132.7, 137.7, 138.7, 139.4, 139.8, 140.0, 165.4, 174.0. HRMS calcd. For $C_{27}H_{28}N_2O_2Se$ $[M+H]^+$: 493.1316, found 493.1389 $[M+H]^+$.

4.2.5.2.2-(2-fluoro-[1,1'-biphenyl]-4-yl)-N-(4-(3-oxobenzo[d][1,2]selenazol-2(3H)-yl)benzyl)propenamide **(5b)**.

Yield: 82 %. White solid. Mp: 97-99°C. ^{1}H NMR (400 MHz, DMSO-6d): δ 1.43 (d, 3H, *J* = 8.00Hz, -CH_3), 3.78 (q, 1H, J = 4.00 Hz, -CH), 4.24-4.36 (m, 2H, -CH_2), 7.27-7.30 (m, 4H, ArH), 7.38-7.41 (m, 1H, ArH), 7.46-7.51 (m, 4H, ArH), 7.54-7.58 (m, 4H, ArH), 7.67-7.71 (m, 1H, ArH), 7.91 (d, 1H, J = 8.00 Hz, ArH), 8.09 (d, 1H, J = 8.00 Hz, ArH), 8.63 (brs, 1H, -NH). ^{13}C NMR (100 MHz, DMSO-6d): δ 18.9, 42.3, 45.1, 115.3 (d, J = 23 Hz), 124.3 (d, J = 3 Hz), 125.1, 126.3, 126.7, 126.9 (d, J = 13Hz), 128.2, 128.4, 128.9, 129.1, 129.2, 130.5 (d, J = 4 Hz), 132.7, 135.,5, 137.6, 138.8, 139.4, 144.5 (d, J = 8 Hz), 158.1, 160.5, 165.5, 173.3. HRMS calcd. For $C_{29}H_{23}FN_2O_2Se$ $[M+H]^+$: 531.0987, found 531.0962 $[M+H]^+$.

4.2.5.3. 2-((2,3-dimethylphenyl)amino)-N-(4-(3-oxobenzo[d][1,2]selenazol-2(3H)-yl)benzyl)benzamide **(5c)**.

Yield: 78 %. White solid. Mp: 110-112°C. ^{1}H NMR (400 MHz, $CDCl_3$): δ 2.20 (s, 3H, -CH_3), 2.32 ((s, 3H, -CH_3), 4.61 (s, 2H, -CH_2), 6.64-6.68 (m, 1H, ArH), 6.75-6.77(m, 1H, ArH), 6.92 (d, 1H, J = 8.00 Hz, ArH), 6.95(d, 1H, J = 8.00 Hz, ArH), 7.05-7.09 (m, 1H, ArH), 7.17-7.23 (m, 2H, ArH), 7.40 (d, 2H, J = 8.00 Hz, ArH), 7.45-7.49 (m, 2H, ArH), 7.58 (d, 2H, J = 8.00 Hz, ArH), 7.63-7.68 (m, 2H, ArH), 8.10 (d, 1H, J = 8.00 Hz, ArH), 9.26 (s, 1H, -NH). ^{13}C NMR (100 MHz, $CDCl_3$): δ 14.0, 20.7, 43.3, 114.9, 116.4, 116.8, 121.1, 123.8, 125.7, 125.8, 126.6, 127.4, 127.5, 128.7, 129.4, 131.1, 132.5, 132.6, 137.0, 137.7, 138.1, 138.3, 139.5, 147.4, 165.9, 169.7. HRMS calcd. For $C_{29}H_{25}N_3O_2Se$$[M+H]^+$: 528.119, found 528.1172 $[M+H]^+$.

4.2.5.4. 2-(3-benzoylphenyl)-N-(4-(3-oxobenzo[d][1,2]selenazol-2(3H)-yl)benzyl)propanamide **(5d)**.

Yield: 80 %. White solid. Mp: 90-92°C. ^{1}H NMR (400 MHz, $CDCl_3$): δ 1.56 (d, 3H, J = 8.00 Hz, -CH_3), 3.68 (q, 1H, J = 8.00 Hz, -CH), 4.35-4.38 (m, 2H, -CH_2), 7.19 (d, 2H, J = 8.00 Hz, ArH), 7.42-7.49 (m, 6H, ArH), 7.56-7.61 (m, 2H, ArH), 7.64-7.66 (m, 3H, ArH), 7.75-7.77 (m, 3H, ArH), 8.06 (s, 1H, -NH). ^{13}C NMR (100 MHz, $CDCl_3$): δ 18.7, 43.1, 46.9, 123.9, 125.7, 126.6, 127.4, 128.4, 128.5, 128.8, 129.1, 129.2, 129.3, 130.1, 131.6, 132.6, 137.0, 137.8, 138.1, 138.2, 141.8, 165.8, 173.6, 196.6. HRMS calcd. For $C_{30}H_{24}N_2O_3Se[M+H]^+$: 541.103, found 541.1001 $[M+H]^+$.

4.2.5.5. (Z)-2-(5-fluoro-2-methyl-1-(4-(methylsulfinyl)benzylidene)-1H-inden-3-yl)-N-(4-(3-oxobenzo[d][1,2]selenazol-2(3H)-yl)benzyl)acetamide **(5e)**.

Yield: 85%. White solid. Mp: 130-132°C. ^{1}H NMR (400 MHz, $CDCl_3$): δ 2.21 (s, 3H, -CH_3), 2.80 (s, 3H, -CH_3), 3.59 (s, 2H, -CH_2), 4.43 (s, 2H, -CH_2), 6.10 (s, 1H, -NH), 6.56-6.61 (m, 1H, ArH), 6.87-6.89 (m, 1H, ArH), 7.16-7.21 (m, 4H, ArH), 7.44-7.52 (m, 3H, ArH), 7.64-7.67 (m, 4H, ArH), 7.70-7.72 (m, 2H, ArH), 8.08 (d, 1H, J = 4.00 Hz, ArH). ^{13}C NMR (100 MHz, $CDCl_3$): δ 10.7, 33.8, 43.1, 43.9, 106.1 (d, J = 23 Hz), 111.3 (d, J = 23 Hz), 123.8, 124.0. 125.7, 126.6, 127.4, 128.5, 128.9, 129.4, 129.6, 130.3, 132.3, 132.7, 136.7, 137.7, 138.3, 138.9, 139.4, 141.4, 145.6, 146.2, 162.2, 164.6, 165.8, 169.2. HRMS calcd. For $C_{34}H_{27}FN_2O_3SSe$ $[M+H]^+$: 643.097, found 643.0956 $[M+H]^+$.

4.2.5.6. 2-(6-methoxynaphthalen-2-yl)-N-(4-(3-oxobenzo[d][1,2]selenazol-2(3H)-yl)benzyl)propanamide **(5f)**.

Yield: 85 %. White solid. Mp: 88-90°C. ^{1}H NMR (400 MHz, DMSO-6d): δ 1.45 (d, 3H, J = 4.00 Hz, -CH_3), 3.82 (q, 1H, J = 4.00 Hz, -CH), 3.86 (s, 3H, -CH_3), 4.27 (s, 2H, -CH_2), 7.13-7.16 (m, 1H, ArH), 7.25 (d, 2H, J =8.00 Hz, ArH), 7.28 (d, 1H, J = 4.00 Hz, ArH), 7.46-7.49 (m, 2H, ArH), 7.52 (d, 2H, J = 8.00 Hz, ArH), 7.66-7.70 (m, 1H, ArH), 7.73 (s, 1H, ArH), 7.76-7.80 (m, 2H, ArH), 7.89 (d, 1H, J = 8.00 Hz, ArH), 8.09 (d, 1H, J = 8.00 Hz, ArH), 8.56 (brs, 1H, -NH). ^{13}C NMR (100 MHz, DMSO-6d):

δ 19.0, 42.2, 45.5, 55.6, 160.2, 119.1, 125.0, 125.8, 126.3, 126.7, 127.0, 127.1, 128.4, 128.8, 128.8, 128.9, 129.6, 132.7, 133.6, 137.7, 137.8, 138.7, 139.4, 157.5, 165.4, 173.9. HRMS calcd. For $C_{28}H_{24}N_2O_3Se[M+H]^+$: 517.103, found 517.1019 $[M+H]^+$.

*4.2.5.7. N-(4-(3-oxobenzo[d][1,2]selenazol-2(3H)-yl)benzyl)-2-((3-(trifluoromethyl)phenyl)amino)benzamide (**5g**)*

Yield: 77%. White solid. Mp: 121-123°C. ^{1}H NMR (400 MHz, DMSO-d_6): δ 1.93 (s, 2H, -CH_2), 6.99 (t, 1H, J = 8.00 Hz, ArH), 7.23 (d, 1H, J = 8.00 Hz, ArH), 7.36-7.43 (m, 6H, ArH), 7.47-7.50 (m, 2H, ArH), 7.58 (d, 2H, J = 8.00 Hz, ArH), 7.68 (t, 1H, J = 8.00 Hz, ArH), 7.78 (d, 1H, J = 8.00 Hz, ArH), 7.90 (d, 1H, J = 8.00 Hz, ArH), 8.09 (d, 1H, J = 8.00 Hz, ArH), 9.20 (brs, 1H, -NH), 9.71 (s, 1H, -NH). ^{13}C NMR (100 MHz, DMSO-d_6): δ 42.6, 114.5 (q, J_{C-F} = 4.0 Hz), 117.4, 117.5 (q, J_{C-F} = 4.0 Hz), 120.4, 121.6, 122.1, 124.2 (q, J_{C-F} = 271 Hz, -CF_3), 125.1, 126.3, 126.7, 128.4, 128.5, 128.9, 129.5, 130.8 (q, J_{C-F} = 32 Hz), 131.0 132.5 (d, J = 22 Hz), 137.5, 138.8, 139.4, 143.1, 143.6, 165.4, 168.9. HRMS calcd. For $C_{28}H_{20}F_3N_3O_2Se[M+H]^+$: 568.0751, found 568.0739 $[M+H]^+$.

*4.2.5.8. 2-(1-(4-chlorobenzoyl)-5-methoxy-2-methyl-1H-indol-3-yl)-N-(4-(3-oxobenzo[d][1,2]selenazol-2(3H)-yl)benzyl)acetamide (**5h**)*

Yield: 82%. White solid. Mp: 91-93°C. ^{1}H NMR (400 MHz, DMSO-6d): δ 2.26 (s, 3H, -CH_3), 3.61 (s, 2H, -CH_2), 3.75 (s, 3H, -OCH_3), 4.30 (s, 2H, -CH_2), 7.72 (d, 1H, J = 4.00 Hz, ArH), 6.97 (d, 1H, J = 8.00 Hz, ArH), 7.15 (s, 1H, ArH), 7.32 (d, 2H, J = 8.00 Hz, ArH), 7.49 (t, 1H, J = 8.00 Hz, ArH), 7.55 (d, 2H, J = 8.00 Hz, ArH), 7.63-7.66 (m, 2H, ArH), 7.69-7.71 (m, 3H, ArH), 7.90 (d, 1H, J = 8.00 Hz, ArH), 8.09 (d, 1H, J = 8.00 Hz, ArH), 8.61 (s, brs, 1H, -NH). ^{13}C NMR (100 MHz, DMSO-6d): δ 13.9, 31.7, 42.4, 55.9, 102.3, 111.9, 114.8, 115.1, 125.0, 126.3, 126.7, 128.4, 128.5, 128.9, 129.5, 130.8, 131.3, 131.6, 132.7, 134.7, 135.7, 137.7, 138.0, 138.8, 139.3, 156.1, 165.5, 168.4, 170.0. HRMS calcd. For $C_{33}H_{26}ClN_3O_3Se[M+H]^+$: 644.0855, found 644.0841 $[M+H]^+$.

4.2.5.9.2-(1,8-diethyl-1,3,4,9-tetrahydropyrano[3,4-b]indol-1-yl)-N-(4-(3-oxobenzo[d][1,2]selenazol-2(3H)-yl)benzyl)acetamide **(5i)**.

Yield: 85%. White solid. Mp: 96-98°C. ^{1}H NMR (400 MHz, DMSO-6d): δ 0.68 (t, 3H, J = 8.00 Hz, -CH_3), 1.25 (t, 3H, J = 8.00 Hz, -CH_3), 2.06 (q, 2H, J = 8.00 Hz, -CH_2), 2.60-2.71 (m, 2H, -CH_2), 2.74-2.78 (m, 1H -CH-), 2.83 (q, 2H, J = 8.00 Hz, -CH_2), 2.91-2.95 (m, 1H -CH-), 3.98 (s, 2H, -CH_2), 4.26-4.35 (m, 2H, -CH_2), 6.88-6.95 (m, 2H, ArH), 7.19 (d, 2H, J = 8.00 Hz, ArH), 7.24 (d, 1H, J = 4.00 Hz, ArH), 7.45 (d, 2H, J = 8.00 Hz, ArH), 7.50 (d, 1H, J = 8.00 Hz, ArH), 7.69 (t, 1H, J = 8.00 Hz, ArH), 7.90 (d, 1H, J = 8.00 Hz, ArH), 8.10 (d, 1H, J = 8.00 Hz, ArH), 8.17 (brs, 1H, -NH), 10.54 (s, 1H, -NH). ^{13}C NMR (100 MHz, DMSO-6d): δ 8.3, 14.9, 22.4, 24.2, 31.1, 42.1, 44.4, 60.4, 76.0. HRMS calcd. For $C_{31}H_{31}N_3O_3Se[M+H]^+$: 574.1609, found 574.1571 $[M+H]^+$.

4.2.5.10. 2-((4-(3-oxobenzo[d][1,2]selenazol-2(3H)-yl)benzyl)carbamoyl)phenyl acetate **(5j)**.

Yield: 82%. White solid. Mp: 112-114°C. ^{1}H NMR (400 MHz, $CDCl_3$): δ 2.14 (3, 3H, -CH_3), 4.59 (d, 2H, J = 4.00 HZ, -CH_2), 6.75 (s, 1H, -NH), 7.09 (d, 1H, J = 8.00 Hz, ArH), 7.29 (t, 1H, J = 8.00 Hz, ArH), 7.39 (d, 2H, J = 8.00 Hz, ArH), 7.46 (t, 2H, J = 8.00 Hz, ArH), 7.60 (d, 2H, J = 8.00 Hz, ArH), 7.64-7.69 (m, 2H, ArH), 7.77 (d, 1H, J = 8.00 Hz, ArH), 8.08 (d, 1H, J = 8.00 Hz, ArH). ^{13}C NMR (100 MHz, $CDCl_3$): δ 20.9, 43.4, 123.3, 123.8, 125.7, 126.4, 126.6, 127.4, 128.2, 128.9, 129.4, 129.8, 132.0, 132.7, 136.7, 137.6, 138.6, 148.0, 165.6, 165.8, 169.3. HRMS calcd. For $C_{23}H_{18}N_2O_4Se[M+H]^+$: 466.0432, found 467.0534 $[M+H]^+$.

*4.2.6. procedure for the synthesis of compound **6***

To a solution of N-Boc-Ethylenediamine (9.0 g) and TEA (6.83 g) in DCM (200 mL) was added o-iodobenzoyl chloride (15.0 g) in portions at 0°C. Then the mixture was stirred at 0°C for 0.5 hour. TLC showed the reaction was complete. Then H_2O (200 mL) was added into the mixture. The aqueous layer was extracted with DCM (20 mL×2), the combined organic layer was washed with brine (50 mL×1), dried over

Na_2SO_4, filtered and the filtrate was concentrated under reduced pressure. The crude product was slurried by MeOH to afford the compound **6** (18.5 g) in 84% yield. ^{1}H NMR (400 MHz, $CDCl_3$): 1.40 (s, 3H, 3-CH_3), 3.36-3.40 (m, 2H, -CH_2), 3.51-3.55 (m, 2H, -CH_2), 5.09 (brs, 1H, -NH), 6.58 (brs, 1H, -NH), 7.05-7.07 (m, 1H, ArH), 7.33-7.35 (m, 2H, ArH), 7.81-7.83 (m, 2H, ArH). ^{13}C NMR (100 MHz, $CDCl_3$): 27.4, 36.5, 52.2, 89.6, 92.8, 127.5, 130.7, 131.2, 141.8, 142.7, 167.8.

*4.2.7. procedure for the synthesis of compound **7***

To a solution of compound **6** (18.5 g) in DMF (180 mL) was added CuI (9.0 g), Cs_2CO_3 (38.66 g), KSeCN (8.19 g) and 1,10-phenanthroline (8.54 g). Then the mixture was stirred at 100 °C for 40 minutes. TLC showed the reaction was complete. The mixture was cooled to 25°C and then diluted with H_2O (400 mL) and EA (200 mL), the aqueous layer was extracted with EA (200 mL×1), the combined organic layer was washed with brine (200 mL×1), dried over Na_2SO_4, filtered and the filtrate was concentrated under reduced pressure. The crude product was slurried by EA to afford compound **7** (7.0 g) as yellow solid in 43.5 % yield. ^{1}H NMR (400 MHz, $CDCl_3$): 1.42 (s, 3H, 3-CH_3), 3.44-3.48 (m, 2H, -CH_2), 3.95-3.98 (m, 2H, -CH_2), 5.03 (brs, 1H, -NH), 7.41-7.45 (m, 1H, ArH), 7.58-7.65 (m, 2H, ArH), 8.03-8.06 (m, 1H, ArH). ^{13}C NMR (100 MHz, $CDCl_3$): 27.6, 39.5, 54.2, 89.4, 127.3, 128.9, 131.4, 132.3, 133.6, 143.4, 170.5.

*4.2.8. procedure for the synthesis of compound **8***

To a solution of compound **7** (300 mg) in DCM (5 mL) was added TFA (1 mL). The mixture was stirred at 25°C for 1 hour. TLC showed the reaction was complete. The mixture was concentrated under reduced pressure to afford crude product 6. The pH of crude product was adjusted to about 9 by TEA. The mixture was used for the next step without purification.

*4.2.9. General procedure for the synthesis of compounds **9a-9j***

To a solution of compound **8** (1.0 eq) in DCM (20 mL) was added EDCI (1.2 eq.), HOBt (1.2 eq), TEA (3.0 eq) and NSAIDs (1.2 eq). The mixture was stirred at 25°C for 16 hrs. TLC showed the reaction was complete. The mixture was diluted with H_2O (20 mL), the aqueous layer was extracted with DCM (15 mL×2), the combined organic layer was washed with brine (15 mL×2), dried over Na_2SO_4, filtered and the filtrate was concentrated under reduced pressure. The crude product was purified by column chromatography on silica gel to afford the desired product.

*4.2.9.1. 2-(4-isobutylphenyl)-N-(2-(3-oxobenzo[d][1,2]selenazol-2(3H)-yl)ethyl)propenamide (**9a**)*

Yield: 80 %. White solid. Mp: 113-115°C. ^{1}H NMR (400 MHz, $CDCl_3$): δ 0.86 (d, 6H, J = 4.00 Hz, 2-CH_3), 1.48 (d, 3H, J = 8.00 Hz, -CH_3), 1.78 (q, 1H, J = 4.00 Hz, -CH), 2.39 (d, 2H, J = 8.00 Hz, -CH_2), 3.50-3.52 (m, 3H, -CH, -CH_2), 3.85-3.97 (m, 1H, -CH), 6.20-6.22 (m, 1H, ArH), 7.01 (d, 2H, J = 8.00 Hz, ArH), 7.16 (d, 2H, J = 8.00 Hz, ArH), 7.42-7.44 (m, 1H, ArH), 7.60-7.61 (m, 1H, ArH), 8.00 (brs, 1H, -NH). ^{13}C NMR (100 MHz, $CDCl_3$): δ 18.3, 22.4, 30.2, 40.2, 44.0, 45.0, 46.7, 124.0, 126.3, 126.7, 127.3, 128.8, 129.5, 132.2, 138.3, 140.6, 168.0, 175.1. HRMS calcd. For $C_{22}H_{26}N_3O_2Se$ $[M+H]^+$: 431.1237, found 431.1209 $[M+H]^+$.

*4.2.9.2. 2-(2-fluoro-[1,1'-biphenyl]-4-yl)-N-(2-(3-oxobenzo[d][1,2]selenazol-2(3H)-yl)ethyl)propanamide (**9b**)*

Yield: 82%. Yellow solid. Mp: 102-104°C. ^{1}H NMR (400 MHz, $CDCl_3$): δ 1.51 (d, 3H, d = 8.00 Hz, -CH_3), 3.54-3.61 (m, 3H, -CH, -CH_2), 3.86-4.03 (m, 2H, -CH_2), 6.62 (brs, 1H, -NH), 7.08-7.12 (m, 2H, ArH), 7.25-7.28 (m, 1H, ArH), 7.34-7.38 (m, 2H, ArH), 7.40-7.48 (m, 4H, ArH), 7.53-7.60 (m, 2H, ArH), 7.97 (d, 1H, J = 8.00 Hz, ArH). ^{13}C NMR (100 MHz, $CDCl_3$): δ 18.3, 40.5, 44.1, 46.5, 115.3 (d, J = 23 Hz), 123.6, 124.1, 126.4, 126.6, 127.7, 128.4, 128.7, 128.9, 130.9, 132.3, 135.5, 138.2, 142.6 158.5, 161.0, 168.2, 174.2. HRMS calcd. For $C_{24}H_{21}FN_2O_2Se$ $[M+H]^+$: 469.083, found 469.0800 $[M+H]^+$.

*4.2.9.3. 2-((2,3-dimethylphenyl)amino)-N-(2-(3-oxobenzo[d][1,2]selenazol-2(3H)-yl)ethyl)benzamide (***9c)**. Yield: 80%. White solid. Mp: 131-133°C. ^{1}H NMR (400 MHz, $CDCl_3$): δ 2.17 (s, 3H, -CH_3), 2.30 (s, 3H, -CH_3), 3.75 (t, 2H, J = 4.00 Hz, -CH_2), 4.11 (t, 2H, J = 4.00 Hz, -CH_2), 6.68 (t, 1H, J = 8.00 Hz, ArH), 6.89 (d, 1H, J = 8.00 Hz, ArH), 6.93 (d, 1H, J = 8.00 Hz, ArH), 7.05 (t, 1H, J = 8.00 Hz, ArH), 7.13-7.20 (m, 2H, ArH), 7.40-7.43 (m, 2H, ArH), 7.52 (d, 1H, J = 8.00 Hz, ArH), 7.56-7.62 (m, 2H, ArH), 9.31 (s, 1H, -NH). ^{13}C NMR (100 MHz, $CDCl_3$): δ 13.9, 20.7, 41.0, 44.4, 114.9, 116.2, 116.9, 120.9, 124.1, 125.6, 125.7, 126.4, 126.6, 127.8, 128.8, 130.9, 132.3, 138.0, 138.3, 139.6, 147.3, 168.4, 170.2. HRMS calcd. For $C_{24}H_{23}N_3O_2Se$ $[M+H]^+$: 466.1033, found 466.0999 $[M+H]^+$.

*4.2.9.4. 2-(3-benzoylphenyl)-N-(2-(3-oxobenzo[d][1,2]selenazol-2(3H)-yl)ethyl)propenamide (***9d)**.

Yield: 82%. White solid. Mp: 116-118°C. ^{1}H NMR (400 MHz, $CDCl_3$): δ 1.53 (d, 3H, J = 8.00 Hz, -CH_3), 3.46-3.60 (m 2H, -CH_2), 3.65 (q, 1H, J = 8.00 Hz, -CH), 3.79-3.86 (m, 1H, -CH-), 3.96-4.02 (m, 1H, -CH-), 6.58 (brs, 1H, -NH), 7.32-7.39 (m, 2H, ArH), 7.47 (t, 2H, J = 8.00 Hz, ArH), 7.54-7.60 (m, 4H, ArH), 7.68 (d, 1H, J = 8.00 Hz, ArH), 7.77-7.79 (m, 3H, ArH), 7.93 (d, 1H, J = 8.00 Hz, ArH). ^{13}C NMR (100 MHz, $CDCl_3$): δ 18.3, 40.6, 44.0, 46.9, 124.2, 126.3, 126.6, 128.4, 128.6, 129.0, 130.2, 131.6, 132.2, 132.7, 137.3, 137.9, 138.4, 141.6, 168.0, 174.2, 196.8. HRMS calcd. For $C_{25}H_{22}N_2O_3Se$ $[M+H]^+$: 479.0874, found 479.0831 $[M+H]^+$.

*4.2.9.5. (Z)-2-(5-fluoro-2-methyl-1-(4-(methylsulfinyl)benzylidene)-1H-inden-3-yl)-N-(2-(3-oxobenzo[d][1,2]selenazol-2(3H)-yl)ethyl)acetamide (***9e)**.

Yield: 82%. White solid. Mp: 127-129°C. ^{1}H NMR (400 MHz, $CDCl_3$): δ 2.33 (s, 3H, -CH_3), 3.52-3.54 (m, 2H, -CH_2), 3.61 (s, 2H, -CH_2), 3.73 (s, 3H, -CH_3), 3.87-3.90 (m, 2H, -CH_2), 6.59 (d, 1H, J = 8.00 Hz, ArH), 6.62 (brs, 1H, -NH), 6.80 (d, 1H, J = 8.00 Hz, ArH), 6.83 (d, 1H, J = 4.00 Hz, ArH), 7.34-7.38 (m, 1H, ArH), 7.45-7.47 (m, 2H, ArH), 7.56-7.60 (m, 2H, ArH), 7.75-7.78 (m, 3H, ArH). ^{13}C NMR (100 MHz, $CDCl_3$): δ 100.8, 112.1, 112.5, 115.1, 124.1, 126.3, 126.4, 128.7, 129.2, 130.4, 131.0, 131.4,

132.3, 133.8, 136.6, 138.0, 139.4, 156.1, 168.0, 168.5, 170.8. HRMS calcd. For $C_{25}H_{29}FN_2O_3SSe$ $[M+H]^+$: 581.0813, found 581.0796 $[M+H]^+$.

*4.2.9.6. 2-(6-methoxynaphthalen-2-yl)-N-(2-(3-oxobenzo[d][1,2]selenazol-2(3H)-yl)ethyl)propanamide (***9f)**.

Yield: 85%. White solid. Mp: 125-127°C. ^{1}H NMR (400 MHz, DMSO-d_6): δ 1.42 (d, 3H, J = 8.00 Hz, -CH_3), 3.32-3.38 (m, 2H, -CH_2), 3.70-3.83 (m, 3H, -CH, -CH_2), 3.85 (s, 3H, -OCH_3), 7.12 (d, 1H, J = 8.00 Hz, ArH), 7.24 (s, 1H, ArH), 7.40-7.44 (m, 2H, ArH), 7.60-7.64 (m, 1H, ArH), 7.69 (d, 2H, J = 8.00 Hz, ArH), 7.74 (d, 1H, J = 8.00 Hz, ArH), 7.82 (d, 1H, J = 8.00 Hz, ArH), 8.03 (d, 1H, J = 8.00 Hz, ArH), 8.20 (brs, 1H, -NH). ^{13}C NMR (100 MHz, DMSO-d_6): δ 18.9, 43.2, 45.7, 55.6, 106.1, 119.0, 125.8, 126.2, 126.3, 127.0, 127.8, 128.2, 128.8, 129.6, 132.0, 133.6, 137.6, 140.0, 157.4, 167.0, 174.3. HRMS calcd. For $C_{23}H_{22}N_2O_3Se$$[M+H]^+$: 445.0874, found 445.0989 $[M+H]^+$.

*4.2.9.7. N-(2-(3-oxobenzo[d][1,2]selenazol-2(3H)-yl)ethyl)-2-((3-(trifluoromethyl)phenyl)amino)benzamide (***9g)**.

Yield: 80%. White solid. Mp: 99-101°C. ^{1}H NMR (400 MHz, $CDCl_3$): δ 3.75 (t, 2H, J = 8.00 Hz, -CH_2), 4.10 (t, 2H, J = 8.00 Hz, -CH_2), 7.18 (d, 1H, J = 4.00 Hz, ArH), 7.28-7.41 (m, 4H, ArH), 7.55-7.62 (m, 4H, ArH), 8.00 (d, 1H, J = 8.00 Hz, ArH), 9.61 (s, 1H, ArH). ^{13}C NMR (100 MHz, $CDCl_3$): δ 41.1, 44.4, 115.9, 116.1 (q, J_{C-F} = 4.0 Hz), 118.2 (q, J_{C-F} = 4.0 Hz), 118.9, 119.3, 122.8, 124.0 (q, J_{C-F} = 271 Hz, -CF_3), 124.1, 126.4, 126.5, 128.2, 128.8, 129.8, 131.6 (q, J_{C-F} = 32 Hz), 132.3 (d, J = 12 Hz), 138.3, 142.5, 144.3, 168.6, 169.8. HRMS calcd. For $C_{23}H_{18}F_3N_3O_2Se$ $[M+H]^+$: 506.0594, found 506.0560 $[M+H]^+$.

*4.2.9.8. 2-(1-(4-chlorobenzoyl)-5-methoxy-2-methyl-1H-indol-3-yl)-N-(2-(3-oxobenzo[d][1,2]selenazol-2(3H)-yl)ethyl)acetamide (***9h)**.

Yield: 80%. White solid. Mp: 116-118°C. ^{1}H NMR (400 MHz, $CDCl_3$): 2.33 (s, 3H, -CH_3), 3.52-3.61 (m, 2H, -CH_2), 3.61 (s, 2H, -CH_2), 3.73 (s, 3H, -OCH_3), 3.87-3.90 (m,

2H, -CH_2), 6.58-6.61 (m, 1H, ArH), 6.62 (brs, 1H, -NH), 6.80 (d, 1H, J = 8.00 Hz, ArH), 6.83 (d, 1H, J = 4.00 Hz, ArH), 7.34-7.37 (m, 1H, ArH), 7.46 (d, 2H, J = 8.00 Hz, ArH), 7.57-7.60 (m, 2H, ArH), 7.75-7.79 (m, 3H, ArH). ^{13}C NMR (100 MHz, $CDCl_3$): δ 13.3, 32.1, 41.0, 43.8, 55.7, 100.8, 112.1, 112.5, 115.1, 124.1, 126.3, 126.4, 128.7, 129.2, 130.4, 131.0, 131.4, 132.3, 133.8, 136.6, 138.0, 139.4, 156.1, 168.0, 168.5, 170.8. HRMS calcd. For $C_{28}H_{24}ClN_3O_4Se$ $[M+H]^+$: 582.0699, found 582.0655$[M+H]^+$.

*4.2.9.9. 2-(3,6-diethyl-1,3,4,5-tetrahydropyrano[4,3-b]indol-3-yl)-N-(2-(3-oxobenzo[d][1,2]selenazol-2(3H)-yl)ethyl)acetamide(***9i)**.

Yield: 85%. White solid. Mp: 87-89°C. ^{1}H NMR (400 MHz, $CDCl_3$): δ 0.74 (t, 3H, J = 8.00 Hz, -CH_3), 1.32 (t, 3H, J = 8.00 Hz, -CH_3), 1.85-1.92 (m, 2H, -CH_2), 2.04-2.09 (m, 2H, -CH_2), 2.76 (q, 2H, J = 8.00 Hz, -CH_2), 2.81-2.88 (m, 2H, -CH_2), 3.56 (q, 2H, J = 8.00 Hz, -CH_2), 3.90-3.98 (m, 2H, -CH_2), 4.00-4.04 (m, 2H, -CH_2), 6.99 (d, 1H, J = 8.00 Hz, ArH), 7.03-7.06 (m, 1H, ArH), 7.17 (brs, 1H, -NH), 7.32 (d, 1H, J = 8.00 Hz, ArH), 7.83-7.42 (m, 1H, ArH), 7.53-7.60 (m, 2H, ArH), 8.00 (d, 1H, J = 8.00 Hz, ArH), 9.52 (s, 1H, -NH). ^{13}C NMR (100 MHz, $CDCl_3$): δ 7.7, 13.9, 22.4, 24.2, 30.9, 40.2, 44.0, 44.6, 60.6, 75.5. 107.9, 115.8, 119.5, 120.2, 124.1, 126.3, 126.4, 126.6, 126.9, 128.8, 132.3, 134.7, 136.1, 138.2, 168.1, 171.9. HRMS calcd. For $C_{26}H_{29}N_3O_3Se$ $[M+H]^+$: 512.1452, found 512.1413 $[M+H]^+$.

4.3. cell viability assay

Five human cancer cell lines BGC-823, SW480, MCF-7, HeLa and A549 cells were maintained in RPMI 1640 medium with 10% fetal bovine serum (FBS) and 100 units/mL of penicillin and streptomycin (Thermo Fisher Scientific, shanghai, China) at 37 °C and 5% CO_2 in a humidified atmosphere. Cells were passaged at preconfluent densities, using a solution containing 0.05% trypsin and 0.5 mM EDTA.

All the tested NSAIDs-EBS derivatives were evaluated in vitro for their cytotoxicity activity against five cancer cell lines by 3-(4,5-dimethylthiazol-2-yl)-2,5-diphenyl-2H-tetrazolium bromide (MTT) assay according to the method as described

before [43]. Exponentially growing cells were harvested and plated in 96-well plates at a concentration of 1×104 cells / well. After 24 h incubation at 37 °C under a humidified 5% CO_2 to allow cell attachment, the cells in the wells were respectively treated with target compounds at various concentrations for 24 h, 48 h and 72 h. The concentration of DMSO was always kept below 1.25%, which was found to be non-toxic to the cells. Three hours prior to experiment termination, MTT solution (20 μL of 5.0 mg/mL solution) was added to each well and incubated at 37°C. At the termination time point, the medium/MTT mixtures were removed, and the formazan crystals formed by the mitochondrial dehydrogenase activity of vital cells were dissolved in 100 μL of DMSO per well. The optical densities were measured at 570 nm using a 96-well multiscanner (Dynex Technologies, MRX Revelation; Chantilly, VA, USA).

4.4. DPPH free radical scavenging activity

DPPH free radical scavenging activity of corresponding compounds was measured according to the method as previous reported with little optimization [44]. Briefly, 20 mL of test samples at different concentrations was mixed with 180 mL of or DPPH solution for 30 min in the dark. Then, the change in absorbance at 517 nm for DPPH was measured on a microplate reader. Ascorbic acid (vitamin C) and ebselen were used as a positive control, DMSO was used as a negative control.

4.5. Bleomycin-dependent DNA damage

The reaction mixture contained DNA (0.5 mg/mL), bleomycin sulfate (0.05 mg/mL), $MgCl_2$ (5 mM), $FeCl_3$ (50 mM), and tested compound in a conc. of 0.1 mg/mL. L-ascorbic acid was used as positive control. The mixture was incubated at 37°C for 1h. The reaction was terminated by addition of 0.05 mL EDTA (0.1 M). The color was developed by adding 0.5 mL TBA (1% w/v) and 0.5 mL HCl (25% v/v), followed by heating at 80°C for 30 minutes. After cooling in ice water, the extent of DNA damage was measured by increase in absorbance at 532 nm [45].

4.6. Glutathione peroxidase-like activity

GPx kit (Biodiagnostic, Egypt) was used for the determination of GPx according to Paglia et al [46]. The reaction mixture contained 1ml assay buffer (50mM phosphate buffer containing 0.1% Triton X-100) and 0.1ml NADPH reagent (24 mmol Glutathione, 12 unit Glutathione reductase and 4.8 mmol NADPH) and 0.01ml (41 mM) tested compounds and the reaction was started by the addition of H_2O_2 (0.8 mM). The contents were mixed well and the absorbances were recorded at 340 nm over a period of 3 min against deionized water. The change of absorbance per minute (A340 nm/min) was estimated using ebselen (41 mM) as positive control. The values represented in Fig 3 are expressed after background correction for the reaction with H_2O_2 and GSH. In case of colored compounds, their activities were estimated after subtracting their own absorbances at the used wave length.

4.7. Colorimetric detection of rat TrxR1 activity

Activity of TrxR1 (Abcam) was assayed using DTNB as substrate. The reactions on 96 well plate were ran in final volume of 100 ml, 100 mM potassium phosphate, pH 7.0, containing 1 mM EDTA, 0.1 mg/ml BSA, 5 nM of TrxR1 and 0.2mM NADPH. Concentration range of compounds for EC_{50} determination was 0.25-25 mM. Reaction mixture was incubated for 15min on plate shaker at room temperature, after which DTNB was added to final concentration of 5 mM. Enzyme kinetics was monitored on TECAN Infinite M1000 PRO microplate reader, by measuring increase in absorbance at 412 nm for 20 min.

4.8. Molecular Modeling

4.8.1 Protein and Ligand Preparation

The mammalian TrxR1 protein (PDB ID: 1H6V) was obtained from Protein Data Bank. The other subunits of TrxR1 were deleted and only one monomer F was prepared by Protein Preparation Wizard in Maestro 11.5 (Schrödinger, LLC, New York, NY, 2019.). Specifically, subunits F was assigned in sequence, hydrogen was added, ionization and tautomerism were adjusted, hydrogen bond distribution was

optimized, water was removed, and structure was minimized. The LigPrep utility in Maestro 11.5 was used to perform ligand preparation applying OPLS2005 force field. The Epik utility is used to generate tautomers and possibly ionized states, and then minimize the resulting 3D conformation.

4.8.2 Ligand Docking

The docking task was completed on Discovery Studio Client 2018. The binding site of TrxR1 was defined as a docking sphere with dimensions X: 27.757, Y: 6.510, Z: 33.698 and R: 15 Å. 10 protein conformations of TrxR1 protein were generated with a maximum alteration of 8 residues, which were typed in CHARMm field force. Under the conformation method FAST, every ligand was generated several conformations. With all other parameters as default, compound **5c** and **5j** were docked into protein structure in the Flexible Docking Protocol. For each pose, the distance between the compound's selenium atom and the sulfur atom of either Cys497 or Cys498 was calculated by the distance monitor in the Discovery Studio. For each ligand, average -CDocker energy and average selenium-sulfur distance were calculated.

Statistical analysis

Data were given as mean ± SD of three independent experiments, graphs and curve fitting were using origin Version 8.0 (OriginLab Corporation, Northampton, USA). P value less than 0.05 was considered statistically significant.

Acknowledgments

This investigation was made possible through the financial support of Shenzhen Fushan Biological Technology Co., Ltd. China.

References

[1] H. Ribeiro, I. Rodrigues, L. Napoleão, L. Lira, D. Marques, M. Veríssimo, J. P. Andrade, M. Dourado, Non-steroidal anti-inflammatory drugs (NSAIDs), pain and aging: Adjusting prescription to patient features, Biomed. Pharmacother. 150 (2022) 112958.

[2] S. Bindu, S. Mazumder, U. Bandyopadhyay, Non-steroidal anti-inflammatory drugs (NSAIDs) and organ damage: A current perspective. Biochem. Pharmacol. 180 (2020) 114147.

[3] S. A. Mirzaei, F. Dinmohammadi, A. Alizadeh, F. Elahian, Inflammatory pathway interactions and cancer multidrug resistance regulation, Life Sci. 235 (2019) 116825.

[4] K. Mortezaee, W. Parwaie, E. Motevaseli, H. Mirtavoos-Mahyari, A. E. Musa, D. Shabeeb, F. Esmaely, M. Najafi, B. Farhood, Targets for improving tumor response to radiotherapy, Int. Immunopharmacol. 76 (2019) 105847.

[5] S. Ramos-Inza, A. C. Ruberte, C. Sanmartín, A. K. Sharma, D. Plano, NSAIDs: old acquaintance in the pipeline for cancer treatment and prevention-structural modulation, mechanisms of action, and bright future, J. Med. Chem. 64 (2021) 16380-16421.

[6] A.P. Fernandes, V. Gandin, Selenium compounds as therapeutic agents in cancer, Biochimica. et. Biophysica. Acta. 1850 (2015) 1642-1660.

[7] D. Basudhar, G. Bharadwaj, R. Y. Cheng, S. Jain, S. Shi, J. L. Heinecke, R. J. Holland, L. A. Ridnour, V. M. Caceres, R. C. Spadari-Bratfisch, N. Paolocci, C. A. Velazquez-Martinez, D. A. Wink, K. M. Miranda, Synthesis and chemical and biological comparison of nitroxyl- and nitric oxide-releasing diazeniumdiolate-based aspirin derivatives, J. Med. Chem. 56 (2013) 7804-7820.

[8] J. L. Williams, N. Nath, J. Chen, T. R. Hundley, J. Gao, L. Kopelovich, K. Kashfi, B. Rigas, Growth inhibition of human colon cancer cells by nitric oxide (NO)-donating aspirin is associated with cyclooxygenase-2 induction and beta-

catenin/T-cell factor signaling, nuclear factor-kappaB, and NO synthase 2 inhibition: implications for chemoprevention, Cancer Res. 63 (2003) 7613-7618.

[9] Y.A. Ammar, M.A. Salem, E.A. Fayed, M.H. Helal, M.S.A. El-Gaby, H. K. Thabet, Naproxen derivatives: Synthesis, reactions, and biological applications，Synth. Commun. 47(15) (2017) 1341-1367.

[10] D. Plano, D. N. Karelia, M. K. Pandey, J. E. Spallholz, S. Amin, A. K. Sharma, Design, synthesis, and biological evaluation of novel selenium (Se-NSAID) molecules as anticancer agents, J. Med. Chem. 59 (2016) 1946-1959.

[11] D. Desai, N. Kaushal, U. H. Gandhi, R. J. Arner, C. D'Souza, G. Chen, H. Vunta, K. El-Bayoumy, S. Amin, K. S. Prabhu, Synthesis and evaluation of the anti-inflammatory properties of selenium-derivatives of celecoxib, Chem. Biol. Interact. 188 (2010) 446-456.

[12] D. Desai, I. Sinha, K. Null, W. Wolter, M. A. Suckow, T. King, S. Amin, R. Sinha, Synthesis and antitumor properties of selenocoxib-1 against rat prostate adenocarcinoma cells, Int. J. Cancer. 127 (2010) 230-238.

[13] A. C. Ruberte, C. Sanmartin, C. Aydillo, A. K. Sharma, D. Plano, Development and therapeutic potential of selenazo compounds, J. Med. Chem. 63 (4) (2020) 1473-1489.

[14] P. Collery, Strategies for the development of selenium-based anticancer drugs, J. Trace Elem. Med. Biol. 50 (2018) 498-507.

[15] C. Sanmartin, D. Plano, A. K. Sharma, J. A. Palop, Selenium compounds, apoptosis and other types of cell death: an overview for cancer therapy, Int. J. Mol. Sci. 13 (8) (2012) 9649-9672.

[16] F. Martini, S. G. Rosa, I. P. Klann, B. C. W. Fulco, F. B. Carvalho, F. L. Rahmeier, M. C. Fernandes, C. W. Nogueira, A multifunctional compound ebselen reverses memory impairment, apoptosis and oxidative stress in a mouse model of sporadic Alzheimer's disease, J. Psychiatr. Res. 109 (2019) 107-117.

[17] D. Bartolini, P. Torquato, M. Piroddi, F. Galli, Targeting glutathione S-transferase P and its interactome with selenium compounds in cancer therapy, Biochim. Biophys. Acta, Gen. Subj. 1863 (2019) 130-143.

[18] S. Kumar, J. J. Yan, J. F. Poon, V. P. Singh, X. Lu, M. K. Ott, L. Engman, S. Kumar, Multifunctional antioxidants: Regenerable radical-trapping and hydroperoxide-decomposing ebselenols, Angew. Chem., Int. Ed. 55 (2016) 3729-3733.

[19] A. J. Pacula, K. B. Kaczor, J. Antosiewicz, A. Janecka, A. Dlugosz, T. Janecki, A. Wojtczak, J. Scianowski, New chiral ebselen analogues with antioxidant and cytotoxic potential, Molecules. 22 (2017) 492.

[20] V. P. Singh, J. F. Poon, J. J. Yan, X. Lu, M. K. Ott, R. J. Butcher, P. J. Gates, L. Engman, Nitro-, azo-, and amino derivatives of ebselen: synthesis, structure, and cytoprotective effects, J. Org. Chem. 82 (2017) 313-321.

[21] D. A. Stoyanovsky, J. F.J iang, M. P. Murphy, M. Epperly, X. L. Zhang, S. Li, J. Greenberger, V. Kagan, H. Bayir, Design and synthesis of a mitochondria-targeted mimic of glutathione peroxidase, mitoebselen-2, as a radiation mitigator. ACS Med. Chem. Lett. 5 (2014) 1304-1307.

[22] L. Liu, S. Li, X. Li, M. Zhong, Y. Lu, J. Yang, Y. Zhang, X. He, Synthesis of NSAIDs-Se derivatives as potent anticancer agents, Med. Chem. Res. 27 (2018) 2071-2078.

[23] Y. Nie, M. Zhong, S. Li, X. Li, Y. Zhang, Y. Zhang, X. He, Synthesis and potential anticancer activity of some novel selenocyanates and diselenides, Chem. Biodivers. 17(5) (2020) e1900603.

[24] X. He, M. Zhong, S. Li, X. Li, Y. Li, Z. Li, Y. Gao, F. Ding, D. Wen, Y. Lei, Y. Zhang, Synthesis and biological evaluation of organoselenium (NSAIDs-SeCN and $SeCF_3$) derivatives as potential anticancer agents, Eur. J. Med. Chem. 208 (2020) 112864.

[25]X. He, Y. Nie, M. Zhong, S. Li, X. Li, Y. Guo, Z. Liu, Y. Gao, F. Ding, D. Wen, Y. Zhang. New organoselenides (NSAIDs-Se derivatives) as potential anticancer agents: Synthesis, biological evaluation and in silico calculations, Eur. J. Med. Chem. 218 (2021) 113384.

[26] S. Bedouhène, F. Moulti-Mati, M. Hurtado-Nedelec, P. M. Dang, J. El-Benna, Luminol-amplified chemiluminescence detects mainly superoxide anion produced by human neutrophils, Am. J. Blood. Res. 7 (2017) 41-48.

[27] B.M. Sahoo, B.K. Banik, P. Borah, A. Jain, Reactive oxygen species (ROS): key components in cancer therapies. Anticancer Agents Med. Chem. 22(2) (2022) 215-222.

[28] J. E. Klaunig, Oxidative stress and cancer, Curr. Pharm. Des. 24 (40) (2018) 4771-4778.

[29] I. Rohn, N. Kroepfl , M. Aschner , J. Bornhorst , D. Kuehnelt , T. Schwerdtle, Selenoneine ameliorates peroxide-induced oxidative stress in C. elegans, J. Trace. Elem. Med. Bio. 55 (2019) 78-81.

[30] G. Bjørklund, M. Shanaida, R. Lysiuk, H. Antonyak, I. Klishch, V. Shanaida, M. Peana, Selenium: an antioxidant with a critical role in anti-aging, Molecules. 27(19) (2022) 6613.

[31] C. P. Kaushik, R. Luxmi, Synthesis, antibacterial, and antioxidant activities of. naphthyl-linked disubstituted 1,2,3-triazoles, J. Heterocycl. Chem. 57 (2020) 2400-2409.

[32] B. Bocchini, B. Goldani, F. S. S. Sousa, P. T. Birmann, C.A. Brüning, E. J. Lenardão, Santi C, Savegnago L, Alves D, Synthesis and antioxidant activity of new selenium-containing quinolines. Med. Chem. 17(6) (2021) 667-676.

[33] A. Sentkowska, K. Pyrzyńska, Investigation of antioxidant activity of selenium compounds and their mixtures with tea polyphenols. Mol. Biol. Rep. 46(3) (2019) 3019-3024.

[34] S.S. Karshieva, G. Babayeva, V. S. Pokrovsky, Y. M. Shlyapnikov, E. A. Shlyapnikova, A. E. Bugrova, A.S. Kononikhin, E. N. Nikolaev, I.L. Kanev, Antitumor effect of bleomycin nanoaerosol in murine carcinoma model. Molecules. 28 (10) (2023) 4157.

[35] U. Galm, M. H. Hager, S.G. Van Lanen, J. Ju, J. S. Thorson, B. Shen. Antitumor antibiotics: bleomycin, enediynes, and mitomycin, Chem. Rev. 105 (2005) 739-758.

[36] Shahabi R, Anissian A, Javadmoosavi SA, Nasirinezhad F, Protective and anti-inflammatory effect of selenium nano-particles against bleomycin-induced pulmonary injury in male rats. Drug. Chem. Toxicol. 44 (1) (2021) 92-100.

[37] L. Flohé, S. Toppo, L. Orian. The glutathione peroxidase family: Discoveries and mechanism. Free Radic. Biol. Med. 187 (2022) 113-122.

[38] R. Gencheva, E. S. J. Arnér, Thioredoxin Reductase Inhibition for Cancer Therapy, Rev. pharmacol. Toxicol. 62 (2022) 177-196.

[39] S. Gromer, L.A. Wessjohann, J. Eubel, W. Brandt, Mutational studies confirm. the catalytic triad in the human selenoenzyme thioredoxin reductase predicted by molecular modeling, Chembiochem. 7 (2006) 1649-1652.

[40] W. Brandt, L. A. Wessjohann, The functional role of selenocysteine (Sec) in the. catalysis mechanism of large thioredoxin reductases: proposition of a swapping catalytic triad including a Sec-His-Glu state, Chembiochem. 6 (2005) 386-394.

[41].E.S.J. Arnér, Targeting the selenoprotein thioredoxin reductase 1 for anticancer therapy. Adv Cancer Res. 136 (2017) 139-151.

[42] S. Shaaban, A. Negm, A. M. Ashmawy, D. M. Ahmed, L. A. Wessjohann. Combinatorial synthesis, in silico, molecular and biochemical studies of tetrazole-derived organic selenides with increased selectivity against hepatocellular carcinoma, Eur. J. Med. Chem. 122 (2016) 55-71.

[43] V. Gandin, P. Khalkar, J. Braude, A.P. Fernandes, Organic selenium compounds as potential chemotherapeutic agents for improved cancer treatment. Free. Radic. Biol. Med. 127 (2018) 80-97.

[44] İ. Gulcin, Antioxidants and antioxidant methods: an updated overview, Arch. Toxicol. 94 (3) (2020) 651-715.

[45] A. B. A. El-Gazzar, M. M. Youssef, A. M. S. Youssef, A. A. Abu-Hashem, F. A. Badria, Design and synthesis of azolopyrimidoquinolines, pyrimidoquinazolines as anti-oxidant, anti-inflammatory and analgesic activities, Eur. J. Med. Chem. 44 (2009) 609-624.

[46] N. M. Giles, G. I. Giles, J. E. Holley, N. J. Gutowski, C. Jacob, Targeting oxidative stress-related diseases: organochalcogen catalysts as redox sensitizers, Biochem. Pharmacol. 66 (2014) 2021-2028.